Proceedings of the International Association for Shell and Spatial Structures (IASS) Symposium 2009, Valencia
Evolution and Trends in Design, Analysis and Construction of Shell and Spatial Structures
28 September – 2 October 2009, Universidad Politecnica de Valencia, Spain
Alberto DOMINGO and Carlos LAZARO (eds.)

Numerical analysis of steel fiber reinforced concrete shells

Tatiana S. A. RIBEIRO*, Pedro SERNA

* Instituto de Ciencia y Tecnología del Hormigón - Universidad Politécnica de Valencia
Camino de Vera s/n, 46022, Valencia, Spain
tasouan@upvnet.upv.es

Abstract

Here, a simple numerical model for steel fiber concrete, based on a reinforced concrete model is presented. In the proposed model concrete is modeled using a finite element dedicated to brittle materials, available at ANSYS library. Fiber contribution to the multiaxial state of concrete is modeled by changing concrete parameters accordingly. Moreover, stress transfer by fiber bridging action is taken in account by considering the fibers as an equivalent smeared reinforcement. An appropriate although simple model for fiber reinforced concrete is therefore obtained by suitably adjusting the parameters of a reinforced concrete model. The proposed model is applied to shells which are part of the Wall of the Benidorm esplanade (Spain). Analyses are carried out on wall segments, considering the structure self-weight, and temperature variations. The numerical results obtained represent well the structural behavior.

Keywords: Steel fiber reinforced concrete, numerical model, commercial program.

1. Introduction

Fiber reinforced concretes (FRC) are composite materials with a cementitious matrix and a discontinuous reinforcement (the fibers). It is known that fibers mainly improve the resistance of the concrete to crack development due to the increase in the material capability of dissipating energy in the cracked regime. Fibers are also particularly suitable to resist impact and fatigue loading, as well as shrinkage cracking.

The earliest applications of FRC were in pavements, in tunnel lining (shotcrete, concrete lining). Nowadays the use of fiber reinforced concrete is increasing in construction industry. The use of fiber reinforcement as partial or total substitution of the traditional reinforcement can be economically convenient, as the higher cost of the material is compensated by a reduction in labor cost.

In the case of structural elements which are not subjected to significant loads, where a minimum reinforcement is required to prevent brittle failure, fibers can be used instead of conventional reinforcement. For thin structures, where placing conventional reinforcement is generally quite difficult, and where meeting the requirements related to the minimum cover is not always possible, discontinuous fibers can suitably substitute conventional reinforcement.

To take most advantage of steel fiber reinforced concrete (SFRC) characteristics, structural design should take into account the stress redistribution on a cracked structure. Nowadays standards for material characterization are available and design guidelines have been proposed. However, a complete model to represent the fiber reinforced concrete is still lacking. It is therefore necessary to obtain a model to analyze complex structures, considering the non-linearity of the material, as well as the structure.

In general, concrete structures are either analyzed by specifically developed finite element based computer programs, or by general purpose codes that provide some kind of material model intended to be employed in the analysis of these structures. Even though the later include finite elements dedicated to concrete, there is no dedicated SFRC element or material law. On the other hand, although having special finite elements and material laws to represent SFRC, the specific finite element codes are in general private codes which are not always available for the research and industry communities.

A numerical model for steel fiber reinforced concrete has been previously presented by Domingo [2] using the commercial software ABAQUS. On that work a specific stress-strain relationship had to be introduced to represent SFRC. The proposed model, presented in details in Ribeiro, Serna and López [6] uses the finite element and material law available for reinforced concrete at ANSYS. The fiber contribution to the multiaxial concrete behavior is considered by changing accordingly the default concrete parameters from ANSYS. Moreover, stress transfer by fiber bridging action is modeled considering the fibers as an equivalent reinforcement smeared on the concrete finite element in three orthogonal directions. Thus, it is possible to obtain a simple model for SFRC by properly adjusting the parameters of the model for reinforced concrete, which gives good assessment on the structural behavior, as shown in Ribeiro, Serna and López [6].

The model obtained previously is briefly presented here and is applied to the analysis of some shells which are part of the Wall of the Benidorm esplanade (Spain). Analyses are carried out on wall segments, considering the structure self-weight, and temperature variations. The numerical results obtained represent well the structural behavior.

2. Numerical Model

The proposed numerical model for the analysis of steel fiber reinforced concrete structures is presented in this section. In addition, comments are made on the main characteristics of the commercial model for reinforced concrete on which the fiber contribution was implemented.

2.1. Numerical Model for Reinforced Concrete

The numerical model for SFRC proposed is based on the models presented by Huang [4] and Padmarajaiah and Ramaswamy [5]. Both models use the software ANSYS that has a finite element dedicated to the analysis of brittle materials. This finite element (SOLID65) considers smeared crack in tension and crushing in compression, and its failure criterion is given by

$$\frac{F}{f_c} - S \geq 0 \tag{1}$$

where F is a function of the principal stresses, S is the Willam and Warnke [8] failure surface, and f_c is the material compressive strength.

When eq.1 is satisfied, the material will crack if any principal stress is tensile and will crush when all principal stresses are compressive. The Willam and Warnke [8] failure surface used in ANSYS is defined by five parameters, which are the concrete uniaxial compressive strength (f_c), concrete tensile strength (f_t), concrete biaxial compressive strength (f_{cb}), concrete biaxial compressive strength superimposed on a hydrostatic stress state (f_1), concrete uniaxial compressive strength superimposed on a hydrostatic stress state (f_2).

Apart from cracking and crushing, SOLID65 can also represent plasticity and creep, and allows the introduction of a reinforcement material in up to three directions. The reinforcement that has uniaxial stiffness and is considered smeared on the concrete finite element, can also present plasticity and creep.

The material model from ANSYS considers perfect bond between reinforcement and concrete. Moreover, ANSYS allows the definition of two shear transfer coefficients, one for opened cracks and the other for closed cracks that are used to model cracks. Concrete cracking is represented by modifying the stress-strain relationship trough the introduction of a failure plane normal to the crack surface. The shear transfer coefficient represents a reduction on the material shear strength that introduces slip trough the crack surface.

2.2. Implementation of fiber contribution

The proposed model is an attempt to join the best characteristics of the models presented by Huang [4] and Padmarajaiah and Ramaswamy [5], commented in a previous paper by Ribeiro et al. [7]. In one hand it keeps the simplicity of Huang's model [4] as only one kind of finite element is used to represent SFRC. On the other hand the fiber contribution to the concrete multiaxial stress state is considered, as done by Padmarajaiah and Ramaswamy [5].

Concrete is modeled on the proponed model using the finite element SOLID65 from ANSYS library, and the Willam and Warnke [8] five-parameter failure criterion. The concrete failure surface is modified accordingly to take into account the fiber contribution to the concrete multiaxial stress state. Concrete parameters f_t and f_c are obtained from experimental results. The other parameters f_{cb}, f_1 and f_2 are defined based on the numerical results from Ribeiro, Serna and Lopez [6] as a function of concrete uniaxial compressive strength, concrete uniaxial tensile strength and concrete flexural-tensile residual strength.

For the shear transfer coefficients, it has been checked in Ribeiro, Serna and López [6] that variations in their values do not change significantly the final solution and their values are therefore defined based on the work by Padmarajaiah and Ramaswamy [5]. Concrete flexural-tensile residual strength is represented according to Huang's model [4]. On the tensile zone ANSYS do not take into account the post-cracking strength for plain concrete (Figure 1). Therefore, to use the software to model SFRC tensile behavior, Huang [4] includes the fibers as an equivalent reinforcement smeared on the concrete finite element. The stress-strain relationship is thus split into two parts: one for plain concrete before cracking and another one post-cracking modified to take into account the fiber contribution (Figure 1).

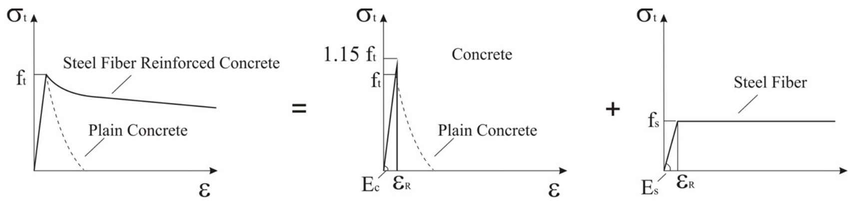

Figure 1: Representation of SFRC model as a combination of plain concrete model and reinforcement model

Cracked concrete finite element is represented by its Young's modulus (E_c) and concrete flexural-tensile residual strength. Concrete flexural strength is increased in 15% to obtain the expected SFRC behavior. The concrete flexural-tensile residual strength is represented as an equivalent reinforcement with cross-sectional area A_s, equivalent Young's modulus (E_s), and equivalent yield strength (f_s). The equivalent reinforcement is modeled using a bilinear model with hardening and von Mises yield criterion. The equivalent reinforcement per concrete finite element is thus obtained as

$$\rho_s = \frac{f_r}{E_s \cdot \varepsilon_R} = \frac{f_r}{\bar{f}_s} \tag{2}$$

where f_r is obtained experimentally following EN-14651 [3]. The equivalent reinforcement is considered smeared on the finite element in three orthogonal directions that coincide with the Cartesian directions.

3. Numerical tests

The proposed numerical model has been initially applied in Ribeiro et al. [7] to some structural elements (Figures 2 to 5), where it has been seen that the model initially proposed should be adjusted. In Ribeiro, Serna and Lopez [6] the model has been adjusted and the parameters used here are the ones considered the best combination of parameters obtained so far for all structural elements analyzed. Concrete parameters obtained experimentally are f_c=43.71MPa, f_t=4.68MPa and f_r=2.9MPa. Concrete Young's modulus and Poisson's ratio are taken as 33000MPa and 0.2, respectively. The other three parameters necessary to obtain the Willam and Warnke [8] failure surface were obtained in Ribeiro, Serna and Lopez [6] and are given by f_{cb}=65.57MPa, f_1=83.31MPa and f_2=148.1MPa. Shear transfer coefficients are assumed to be β_t=0.45 and β_c=0.76 for opened and closed cracks, respectively. For the fibers, the equivalent reinforcement has as parameters the Young's modulus E_s=2000000MPa, Poisson ratio ν=0.3, equivalent yield strength f_s=1650MPa, and the concrete flexural-tensile residual strength obtained experimentally is used to determine the equivalent reinforcement per concrete finite element, as shown in eq.2.

Figures 2 to 5 show the numerical results obtained from the application of the proposed model with the aforementioned parameters to four structural elements, where two of them are standard tests, compared to the experimental results. It can be seen from Figures 2 to 5 that the proposed model gives a good assessment on the experimental behavior for serviceability state. For limit state, results obtained with the proposed model are on the safety side.

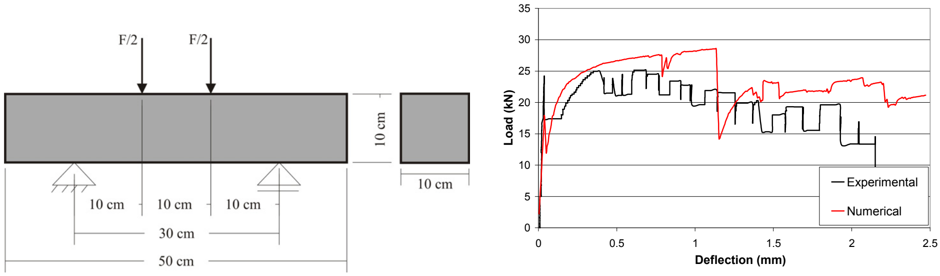

Figure 2: Test from ASTM1018 [1] – Geometry, load conditions and results

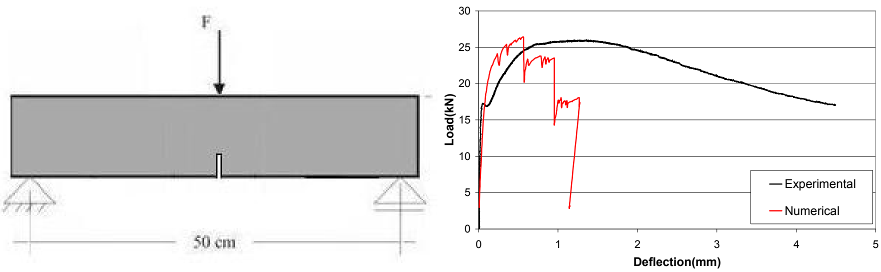

Figure 3: Test from EN14651 [3] – Geometry, load conditions and results

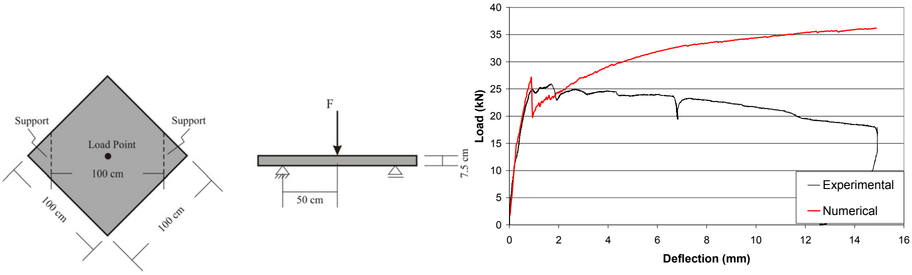

Figure 4: Plate with a central load – Geometry, load conditions and results

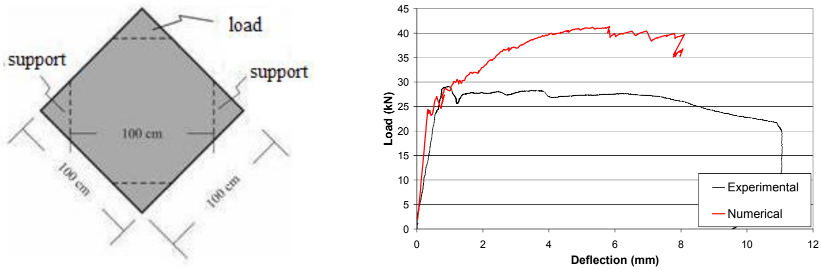

Figure 5: Plate with two line loads – Geometry, load conditions and results

4. Analysis of Benidorm esplanade wall

On the re-urbanization project of the West Beach in Benidorm (Spain), developed by the Infrastructures Department of the Valencian Government the execution of a 4m high wall along 1300m of the beach, defining the maritime facade has been included, by taking into account all required aesthetic criteria.

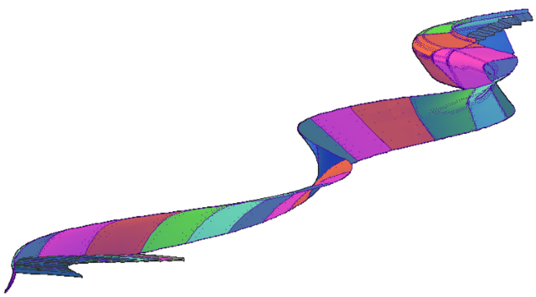

Figure 6: Scheme of the wall

The shape of the facade generates a surface with double curvature in following the original project by Ferraté and Martí (Figure 6). This wall has no properly retaining or load transmission functions. However, self-weight loads are expected to produce stresses beyond plain concrete capacity under tension. Due to the shells geometry, placement of conventional reinforcement is really complicated. This is one of the cases, as commented on the introduction, where the substitution of conventional reinforcement by fibers is highly recommended. The structural design should therefore consider the fiber contribution. A numerical analysis considering both the material and the structure non-linearity should be performed.

The structure was analyzed in segments with approximately 5m in length, resting on lateral buttresses. Each wall segment was analyzed under the double of its self-weight and under temperature variations of $\pm$ 20 ºC, where these loads are applied separately.

At first linear elastic analyzes were performed using the finite element (SOLID45) ANSYS library. Figure 7a shows the results from the first principal stress obtained for one wall segment under the double of its self weight. It can be noticed that the higher tensile stresses appear in the upper edges of the top surface of the segment, reaching values of 2.8MPa. Figure 7b shows the results for the same segment under a temperature variation of +20 ºC, where it tensile stresses reach 5.0MPa. For a negative temperature variation the situation is even more critical, and tensile stresses reach 19.39MPa. It is clear from these results that cracks will appear on the structure.

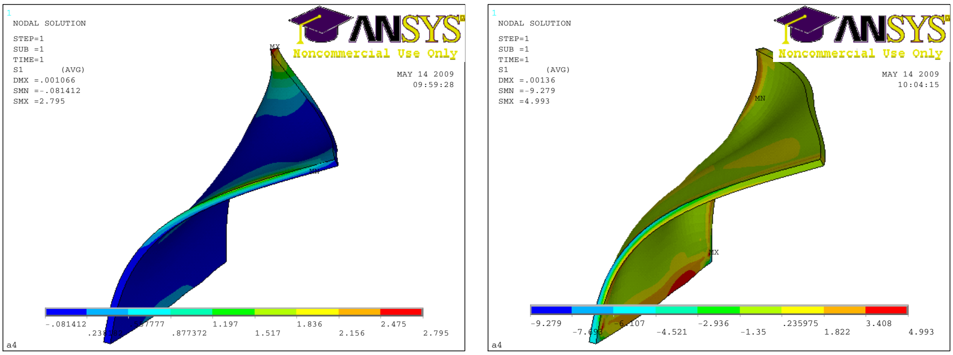

(a) (b)

Figure 7: Principal Stresses from linear elastic analysis – double segment self-weight (a) and positive temperature variation (b)

In order to verify the contribution of the fibers to the structural behavior, a non-linear numerical analysis is performed. Steel fiber reinforced concrete without conventional reinforcement is considered in the whole structure. The numerical model presented in section 2 is used with the following concrete parameters: E_c=27300MPa, ν=0.2, f_c=21.2MPa, f_t=2MPa, f_r=1MPa, f_{cb}=31.8MPa, f_1=40.41MPa and f_2=71.83MPa. For the equivalent reinforcement (the fibers), the parameters used are E_s=2000000MPa, ν=0.3 and f_s=1650MPa. As for the shear transfer coefficients the following values are used: β_t=0.2 and β_c=0.4. Figure 8a shows the first principal stresses considering double the segment self-weight.

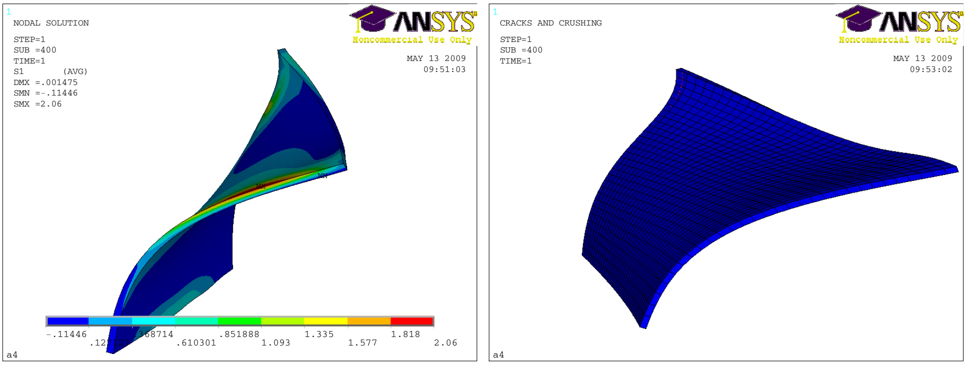

(a) (b)

Figure 8: Principal Stresses (a) and Cracks (b) from non-linear analysis – double segment self-weight

Due to stress redistribution post-cracking, the maximum tensile stress obtained is 2.06MPa. The cracked area is restricted to few finite elements on the upper edge of the wall, near to the buttress, as shown in Figure 8b, where the cracked elements are marked with red points. Although the smeared crack model does not provide crack dimensions, an estimate of the maximum crack opening ought to occur can be obtained by the product between the elemental strain and the finite element size, as

$$\delta = \varepsilon \cdot \ell \tag{3}$$

where δ is the crack opening, ε is the total elemental mechanical and thermal strain, and ℓ is the element biggest dimension. Here it has been considered that only one crack appears in each element, as this would be the most unfavorable situation. Using this equation the estimated crack opening obtained is 0.28mm in the case of double segment self-weight. Figure 9 shows the first principal strain for double the segment self-weight, where it can be seen that the higher crack is located on a single finite element near the lateral buttress.

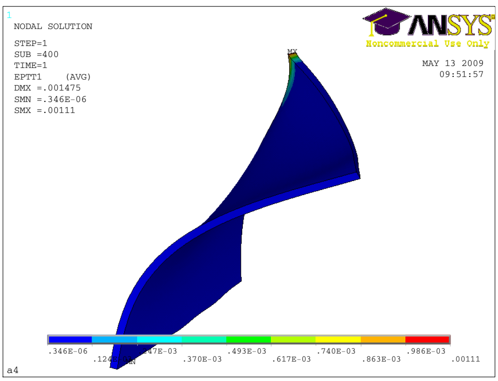

Figure 9: Principal strain from non-linear analysis – double segment self-weight

As for positive temperature variation, principal stresses of up to 2.36MPa are obtained (Figure 10a), which leads to a maximum estimated crack opening of 1.5mm. This maximum crack is located on a single finite element at the upper edge of the shell near the buttresses, as can be seen in Figure 10b. Other important cracks are also located near the buttresses and are restricted to a line of finite elements. Although the shell presents some cracks on other zones these are much smaller and can be accepted (Figure 11).

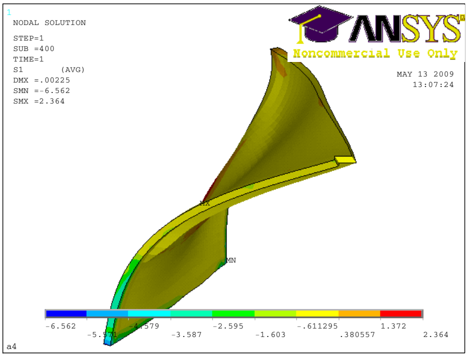

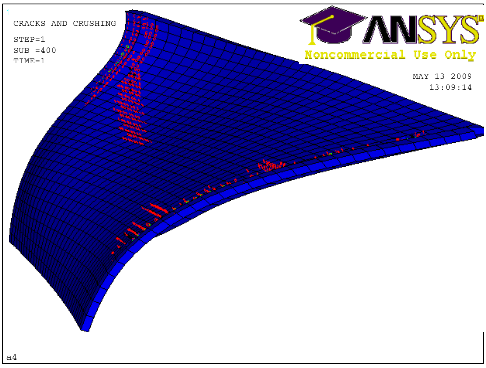

(a) (b)

Figure 10: Principal stress and cracks from non-linear analysis – positive temperature variation

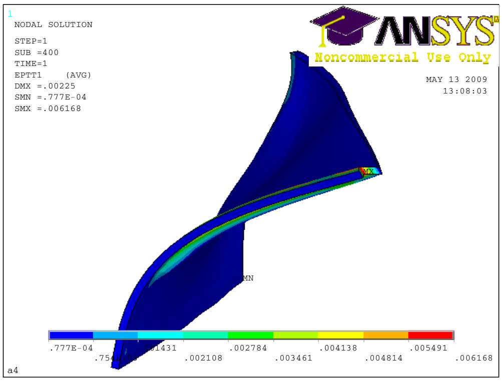

Figure 11: Principal strain from non-linear analysis – positive temperature variation

Regarding negative temperature variation, maximum principal tensile stresses are about 1.93MPa (Figure 12a). Analogous to positive temperature variation, the higher cracks are located near the buttresses, as shown in Figure 12b, and their maximum estimated opening reaches 0.35mm. This high crack is located on a single finite element. Much smaller cracks can be observed on other shell zones (Figure 13).

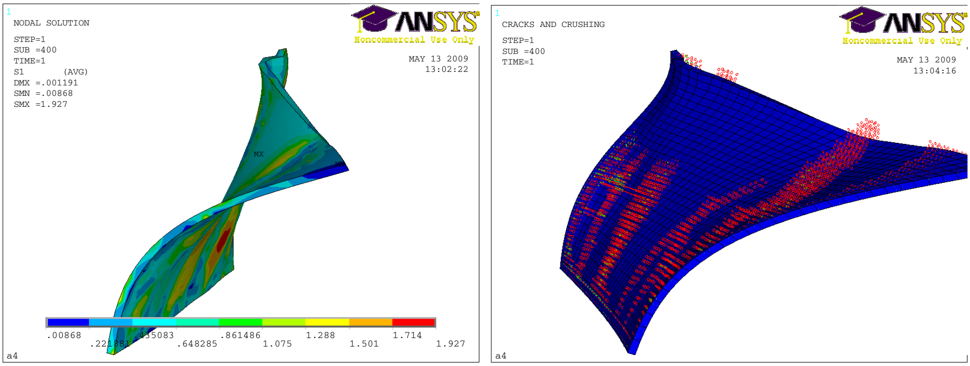

(a) (b)

Figure 12: Principal stresses (a) and cracks (b) from non-linear analysis – negative temperature variation

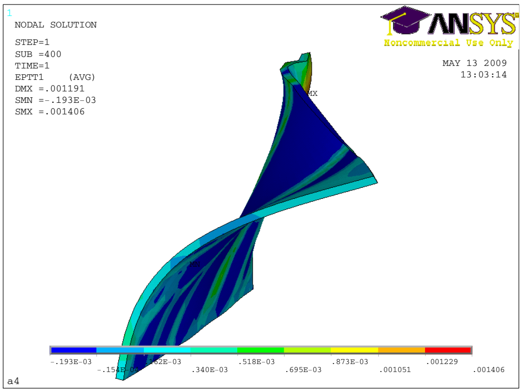

Figure 13: Principal strain from non-linear analysis – negative temperature variation

As on the original structural design a concrete reinforced with a mesh of 8mm bars each 10 cm in the midsection of the wall was proposed, another analysis was conducted considering this solution. The structure thickness was divided into three layers of 4cm each to perform the numerical analysis, as shown in Figure 14. The exterior layers, blue in the figure, are of plain concrete, whose parameters are E_c=27300MPa, ν=0.2, f_c=21.2MPa, f_t=2MPa, f_{cb}=25.44MPa, f_1=30.74MPa and f_2=36.57MPa. The mid layer of the shell, purple in Figure 14, is of reinforced concrete. In this layer concrete has the same parameters of the exterior layers, however it contains steel bars which are considered smeared on the concrete finite element in two directions, which would be the directions of the rebar mesh. Steel reinforcement follows von Mises yield criterion with parameters E_s=200000MPa, ν=0.3 and f_s=500MPa.

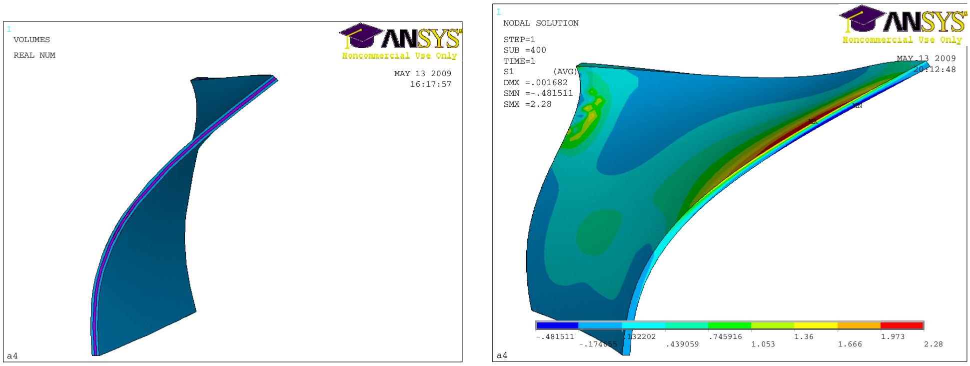

(a) (b)

Figure 14: Analysis with conventional reinforcement – geometry of the shell (a) and principal stresses (b)

Results obtained for principal strains and cracks under double the segment self-weight are shown in Figure 15a, where it can be seen that strains up to 3.47‰ are obtained, which would lead to a maximum estimated crack opening of 0.87mm. These cracks appear on the upper corner near the lateral buttress. Therefore, this solution is more unfavorable than the use of fibers. For temperature variations the situation is even more critical, presenting more cracks, as can be seen in Figure 15b, and higher strains which would lead to high crack openings.

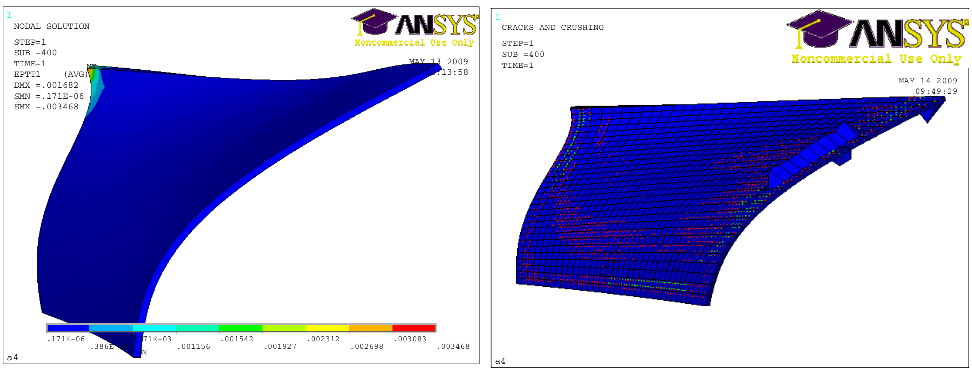

(a) (b)

Figure 15: Analysis with conventional reinforcement – principal strain for double segment self-weight (a) and cracks for positive temperature variation (b)

4. Conclusions

A numerical model for the analysis of SFRC structures has been presented, where a commercial finite element model for reinforced concrete is properly adjusted to represent the material behavior. The proposed model has been validated on simple structural elements. The numerical solutions for such elements were compared with experimental results, and it has been seen that a good assessment on the structural behavior can be obtained with the proposed model.

The application of the model to the analysis of the shells from the Wall of Benidorm esplanade shows that the use of fiber in this case is really interesting. A significant gain in structural performance is obtained as thinner and fewer cracks appear on the structure compared to the cracks that appear when conventional reinforced concrete is used. Moreover, the use of steel fibers in this structure would require less labor work.

Acknowledgement

The authors would like to acknowledge the financial support received from the Spanish "Ministerio de Educación y Ciencia", project SB2006-0121. Moreover, we want to express our most sincere gratitude to Vicente Ibarra and the Conselleria d'Infrastructures i Transports of the Valencian Government, in acknowledgement of the possibility to work in the Benidorm Esplanade.

References

[1] ASTM C 1018, Standard test method for flexural toughness and first crack strength of fiber reinforced concrete (using beam with third-point loading). *Annual book of ASTM Standards*, 1997, 04.02.

[2] Domingo A.C., *Estudio del comportamiento del hormigón con fibras de acero en elementos laminares de pequeño espesor y su comportamiento post-fisuración*, Departamento de Ingeniería de la Construcción y Proyectos de Ingeniería Civil, Universidad Politécnica de Valencia, PhD Thesis, 2000.

[3] EN 14651. Test Method for Metallic Fibered Concrete - Measuring the Flexural Tensile Strength. *European Standards*, 2005.

[4] Huang Z., *Grenzbeanspruchung gebetter Stahlfaserbetonplatten*, Institut für Baustoffe, Massivbau und Brandschutz, TU Braunschweig, PhD Thesis, 1995.

[5] Padmarajaiah S.K. and Ramaswamy A., A finite element assessment of flexural strength of prestressed concrete beams with fiber reinforcement. *Cement and Concrete Composites*, 2002; **24**; 229-241.

[6] Ribeiro T.S.A., Serna P. and López A. M. N., Implementación de la contribución de fibras en modelos numéricos comerciales para hormigón estructural, in *Congreso de Métodos Numéricos en Ingeniería*, 2009, to appear.

[7] Ribeiro T.S.A., Serna P., Ribeiro G.O. and López A. M. N., Numerical modeling of steel fiber reinforced concrete structures, in *7th RILEM International Symposium on Fiber Reinforced Concrete: Design and Applications*, Gettu R (ed), RILEM publications, 2008, 345-356.

[8] Willam K.J. and Warnke E.P., Constitutive model for triaxial behaviour of concrete. *Structural Engineering International*, 1975; **19**; 1-30.